CHEMICAL ENGINEERING TRANSACTIONS
VOL. 62, 2017
A publication of AIDIC
The Italian Association of Chemical Engineering
Online at www.aidic.it/cet
Guest Editors: Fei Song, Haibo Wang, Fang He

ISBN 978-88-95608- 60-0; **ISSN** 2283-9216
DOI: 10.3303/CET1762200

Impact of Crowbar Resistances on Low Voltage Ride Through of Doubly Fed Induction Wind Turbine Generation System

Wenjuan Zhang[a], Haomiao Ma[b], Feige Zhang[a]

[a]School of Electrical Engineering, Baoji University of Arts and Sciences, Baoji 721016, China
[b]School of Computer Science, Shaanxi Normal University, Xi'an 710062, China
wenjuanzhang@163.com

The impact of crowbar resistance on low voltage ride through (LVRT) of doubly-Fed induction generator (DFIG) is researched. The relationship between the crowbar resistance and the rotor transient current and the attenuation rate of stator rotor transient flux is derived. It is proposed to add series dynamic capacitor in crowbar circuit to decrease the absorbed reactive power. Results show that, either too large or too small crowbar resistance may weaken the ability of DFIG LVRT, the optimal crowbar resistance should be selected and the additional dynamic capacitor makes the rotor overcurrent has a smaller transient time constant and a faster recovery speed for the grid fault.

1. Introduction

In the past decades, doubly-fed induction generators (DFIG) has increased significantly due to advantages of variable speed constant frequency (VSCF) operation, decoupled control of active and reactive power and enjoy partial-scale converters (Mohsen and Mostafa, 2010). However, since the stator of the DFIG is directly connected to the grid, thus, the promising wind generator technology is vulnerable to grid disturbances(Mikel et al., 2012).It is desired that the wind turbines remain connected to the grid and actively contribute to the system stability during and after grid voltage sag faults and disturbances, this ability of wind turbines is termed as low voltage ride through (LVRT) capability (Vinothkumar and Selvan, 2011).One effective way to make the DFIG have the capability of LVRT is to equipped with appropriate crowbar protection circuit in the rotor side of the DFIG(Niiranen, 2004). Niiranen analyzes the DFIG equivalent circuit and points out that an appropriate crowbar resistance is helpful for LVRT. Based on an analysis of the characteristics of stator and rotor fault currents (Niiranen, 2004), further analyzed the effect of a DC bus clamp on DFIG short-circuit current, and put forward a selection method for the crowbar resistance (Xu et al., 2010).
Based on this, the paper aiming at the fault of three-phase symmetrical voltage sag at the grid, firstly, the impact on DFIG operation characteristics and transient flux attenuation of crowbar resistance is analyzed by mathematical method. Secondly, the reactive power absorbed by DFIG is discussed when the crowbar is in operation and it is proposed to add a series additional dynamic capacitance to reduce reactive power absorbed from the grid, promoting a rapid recovery of fault voltage. Finally, the system simulation is done in the 3MW wind power generation simulation platform.

2. Mathematical model of DFIG before grid faults

The stator and rotor voltages and fluxes in a stationary reference frame are given as.

$$\begin{cases} \boldsymbol{u}_{\mathrm{s}} = R_{\mathrm{s}}\boldsymbol{i}_{\mathrm{s}} + \dfrac{\mathrm{d}\boldsymbol{\psi}_{\mathrm{s}}}{\mathrm{d}t} + \mathrm{j}\omega_{\mathrm{s}}\boldsymbol{\psi}_{\mathrm{s}} \\ \boldsymbol{u}_{\mathrm{r}} = R_{\mathrm{r}}\boldsymbol{i}_{\mathrm{r}} + \dfrac{\mathrm{d}\boldsymbol{\psi}_{r}}{\mathrm{d}t} + \mathrm{j}(\omega_{\mathrm{s}} - \omega_{\mathrm{r}})\boldsymbol{\psi}_{\mathrm{r}} \end{cases} \tag{1}$$

Please cite this article as: Wenjuan Zhang, Haomiao Ma, Feige Zhang, 2017, Impact of crowbar resistances on low voltage ride through of doubly fed induction wind turbine generation system, Chemical Engineering Transactions, 62, 1195-1200 DOI:10.3303/CET1762200

$$\begin{cases} \boldsymbol{\psi}_{\mathrm{s}} = L_{\mathrm{s}}\boldsymbol{i}_{\mathrm{s}} + L_{\mathrm{m}}\boldsymbol{i}_{\mathrm{r}} \\ \boldsymbol{\psi}_{\mathrm{r}} = L_{\mathrm{m}}\boldsymbol{i}_{\mathrm{s}} + L_{\mathrm{r}}\boldsymbol{i}_{\mathrm{r}} \end{cases} \tag{2}$$

In these equations, all parameters are reduced to the stator side. where, us□[usd usq] T and ur□[urd urq] T are the stator and rotor voltage vector, is□[isd isq] T and ir□[ird irq]T are the stator and rotor current vector, □s□[□sd □sq]T and□□r□[□rd □rq]T are the stator and rotor flux vector, Ls and Lr are the stator and rotor self-inductances, Lm is the mutual inductance. ωs is the stator slip frequency, ωr is the rotor slip frequency. Also, Rs and Rr are the stator and rotor resistances.

Before the occurrence of a voltage dip, i.e. t□t0, the stator voltage space vector is a vector of constant amplitude u0 that rotates at synchronous electrical angular frequency □s, and so, the stator voltage space vector can be described as

$$\boldsymbol{u}_{\mathrm{s}} = u_0 \mathrm{e}^{\mathrm{j}\omega_{\mathrm{s}} t} \tag{3}$$

By substituting Equ. (2) into (1), the stator voltage oriented is used, per unit □s□1, the slip s□(□s□□r)/□s□1□□r, the steady rotor current before voltage dip is yields as:

$$\boldsymbol{i}_{\mathrm{r}(0\_)} = \frac{\frac{L_{\mathrm{s}}}{s}\sqrt{u_{\mathrm{rd}}^2 + u_{\mathrm{rq}}^2}\,\mathrm{e}^{\mathrm{j}\theta t} + L_{\mathrm{m}}u_0}{\mathrm{j}(L_{\mathrm{s}}L_{\mathrm{r}} - L_{\mathrm{m}}^2)} \tag{4}$$

where,$\theta = \arctan(u_{rq}/u_{rd})$

The stator resistance can be neglected in steady state. Based on (2) and (3), the expressions for the stator flux and rotor flux in steady state are obtained as:

$$\boldsymbol{\psi}_{\mathrm{s}(0\_)} = \frac{u_0 \mathrm{e}^{\mathrm{j}\omega_{\mathrm{s}} t}}{\mathrm{j}\omega_s}, \boldsymbol{\psi}_{\mathrm{r}(0\_)} = \frac{u_0 \mathrm{e}^{\mathrm{j}(1-s)\omega_{\mathrm{s}} t}}{\mathrm{j}\omega_{\mathrm{s}}} \tag{5}$$

3. Impact of crowbar resistances on operation characteristics of DFIG

3.1 Impact on rotor current

Rotor current after voltage dip consists of two components: the first is transient attenuation component that caused by grid voltage dip, the second is steady state current attenuation component.

For the transient attenuation component, at time t□t0, a three-phase dip fault is assumed to occur at the stator of the DFIG, according to Equ. (3), the stator voltage are:

$$\boldsymbol{u}_{\mathrm{s}} = \begin{cases} u_0 \mathrm{e}^{\mathrm{j}\omega_{\mathrm{s}} t} & t < t_0 \\ (1-p)u_0 \mathrm{e}^{\mathrm{j}\omega_{\mathrm{s}} t} & t \geq t_0 (0 \leq p \leq 1) \end{cases} \tag{6}$$

Where p is the voltage dip ratio. This implies that the flux in both the windings does not change. The stator and rotor flux are given by

$$\boldsymbol{\psi}_{\mathrm{s}(0)} = \boldsymbol{\psi}_{\mathrm{r}(0)} = pu_0 / (\mathrm{j}\omega_{\mathrm{s}}) \tag{7}$$

This transient flux will be decayed with the form of exponent, the damping time constant of the dc components in stator and rotor can be defined as

$$T_{\mathrm{s}}^{'} = \frac{L_{\mathrm{s}(0_+)}}{R_{\mathrm{s}}} \tag{8}$$

$$T_{r}^{'} = \frac{L_{\mathrm{r}(0_+)}}{R_r} \tag{9}$$

In these equations, the transient stator inductance can be derived as

$$L_{\mathrm{s}(0_+)} = L_{\mathrm{s}} + \frac{L_{\mathrm{r}}L_{\mathrm{m}}}{L_{\mathrm{r}} + L_{\mathrm{m}}} \tag{10}$$

Similarly, the transient rotor inductance can be introduced as

$$L_{\mathrm{r}(0_+)}=L_{\mathrm{r}}+\frac{L_{\mathrm{s}}L_{\mathrm{m}}}{L_{\mathrm{s}}+L_{\mathrm{m}}} \tag{11}$$

Thus, the change of stator and rotor flux after the voltage dip could be expressed mathematically in rotor reference frame as follows

$$\begin{cases}\psi_{\mathrm{s}(0_+)}=\psi_{\mathrm{s}(0)}\mathrm{e}^{-\frac{t}{T_s'}}=\dfrac{pu_0\mathrm{e}^{-\mathrm{j}(1-s)\omega_s t}}{\mathrm{j}\omega_s}\mathrm{e}^{-\frac{t}{T_s'}}\\ \psi_{\mathrm{r}(0_+)}=\psi_{\mathrm{r}(0)}\mathrm{e}^{-\frac{t}{T_r'}}=\dfrac{pu_0}{\mathrm{j}\omega_s}\mathrm{e}^{-\frac{t}{T_r'}}\end{cases} \tag{12}$$

And the detailed analysis of the transient rotor current, $i_r^1(0_+)$, $i_r^2(0_+)$ inductived by transient flux, $\psi_s(0_+)$ $\psi_r(0_+)$ can be found, where this will no longer be further described. We only give the dynamic current expression as follows

$$\begin{cases}\boldsymbol{i}_{\mathrm{r}(0_+)}^1=-\dfrac{\psi_{\mathrm{s}(0_+)}L_{\mathrm{m}}}{L_{\mathrm{s}(0_+)}(L_{\mathrm{r}}+L_{\mathrm{m}})}\\ \boldsymbol{i}_{\mathrm{r}(0_+)}^2=\psi_{\mathrm{r}(0_+)}/L_{\mathrm{r}(0_+)}\end{cases} \tag{13}$$

By substituting Equ.(12) into (13), the general transient rotor current is thus given by

$$\boldsymbol{i}_{\mathrm{r}(0_+)}=\boldsymbol{i}_{\mathrm{r}(0_+)}^1+\boldsymbol{i}_{\mathrm{r}(0_+)}^2=\frac{pu_0}{\mathrm{j}\omega_s}\left(\frac{\mathrm{e}^{-\frac{t}{T_r'}}}{L_{\mathrm{r}(0_+)}}-\frac{L_{\mathrm{m}}\mathrm{e}^{-\mathrm{j}(1-s)\omega_s t}\mathrm{e}^{-\frac{t}{T_s'}}}{L_{\mathrm{r}}L_{\mathrm{s}(0_+)}}\right) \tag{14}$$

For the steady state current attenuation component $i_{r(0++)}$, based on (4), the term can be written as

$$\boldsymbol{i}_{\mathrm{r}(0_{++})}=\boldsymbol{i}_{\mathrm{r}(0_-)}\mathrm{e}^{-\frac{t}{T_r'}} \tag{15}$$

So, by adding Eqs. (14) and (15), the final expression of rotor currents during voltage dip can be written as following

$$\boldsymbol{i}_{\mathrm{r}(0_+)\mathrm{sum}}=\boldsymbol{i}_{\mathrm{r}(0_+)}+\boldsymbol{i}_{\mathrm{r}(0_{++})}=\frac{pu_0}{\mathrm{j}\omega_{\mathrm{s}}}\left(\frac{\mathrm{e}^{-\frac{t}{T_r'}}}{L_{\mathrm{r}(0_+)}}-\frac{L_{\mathrm{m}}\mathrm{e}^{-\mathrm{j}(1-s)\omega_s t}\mathrm{e}^{-\frac{t}{T_s'}}}{L_{\mathrm{r}}L_{\mathrm{s}(0_+)}}\right)+\frac{\frac{L_{\mathrm{s}}}{s}\sqrt{u_{rd}^2+u_{rq}^2}\mathrm{e}^{\mathrm{j}\theta t}+L_{\mathrm{m}}u_0}{\mathrm{j}(L_{\mathrm{s}}L_{\mathrm{r}}-L_{\mathrm{m}}^2)}\mathrm{e}^{-\frac{t}{T_r'}} \tag{16}$$

According to Eqs. (16), on the one hand, although the current vector does not reach the maximum value exactly at t = T/2, the current after half a period gives a good approximation of the maximum current. On the other hand, after the crowbar is in operation, the rotor current damping time constant T_r' becomes T_{rcb}'

$$T_{rcb}^{'}=\frac{L_{\mathrm{r}(0_+)}}{R_r+R_{cb}} \tag{17}$$

As shown by Eqn. (17), the rotor current damping time constant become smaller after the crowbar is in operation. Therefore, during the LVRT process of DFIG turbine generation system, the larger the crowbar resistance, the smaller transient rotor current.

3.2 Impact on stator and rotor flux

In order to derive the relationship between the flux and crowbar resistance, according to Eqn. (1) and (2), the grid voltage is selected as the input variable, the stator and rotor flux as state variables, with the stator and rotor current as output variables. Consequently, the state equation based mathematical model of the DFIG is rewritten as

$$\begin{cases} \dfrac{d\boldsymbol{\psi}}{dt} = \boldsymbol{A\psi} + \boldsymbol{u} \\ \boldsymbol{i} = \boldsymbol{L}^{-1}\boldsymbol{\psi} \end{cases} \tag{18}$$

Where u is the grid voltage vector, i is the current vector, and □□ is the flux vector.
The system matrix A and output matrix L^{-1} can be defined as

$$\boldsymbol{A} = \begin{bmatrix} -\sigma_s & \omega_s & \sigma_{sm} & 0 \\ -\omega_s & -\sigma_s & 0 & \sigma_{sm} \\ \sigma_{rm} & 0 & -\sigma_r & (\omega_s - \omega_r) \\ 0 & \sigma_{rm} & -(\omega_s - \omega_r) & -\sigma_r \end{bmatrix}, \boldsymbol{L}^{-1} = \frac{1}{L_s L_r - L_m^2} \begin{bmatrix} L_r & 0 & -L_m & 0 \\ 0 & L_r & 0 & -L_m \\ -L_m & 0 & L_s & 0 \\ 0 & -L_m & 0 & L_s \end{bmatrix},$$

Where $\sigma_{sm} = \frac{R_s L_m}{L_s L_r - L_m^2}$ and $\sigma_{rm} = \frac{R_r L_m}{L_s L_r - L_m^2}$reflect the impact on the stator and rotor flux. As the stator and rotor resistance is usually small, σ_{sm} and σ_{rm} can be considered to approximate zero. In this model, $\sigma_s = \frac{R_s L_r}{L_s L_r - L_m^2}$ and $\sigma_r = \frac{R_r L_s}{L_s L_r - L_m^2}$ reflect the stator and rotor flux transient attenuation rates respectively. Hence when the grid voltage sags, the stator flux is a dc component in the stator reference frame and is attenuated with the rate of σ_s; in the synchronous rotating coordinate frame, the stator flux is an ac component oscillating at $(\omega_s - \omega_r)$ and is attenuated by the rate of σ_s. Similarly, the rotor flux is a dc component in the rotor reference frame and is attenuated by the rate of σ_r; in the synchronous rotating reference frame, the rotor flux is an ac component oscillating at $(\omega_s - \omega_r)$ and is attenuated by the rate of σ_r.
During grid voltage sag and recovery, the transient component of the DFIG stator flux is the main cause of rotor overcurrent and overvoltage. According to the above analysis, the stator transient flux attenuation rate σ_s influences whether or not the crowbar is in operation. When the voltage dip has occurred, and the rotor overcurrent is large enough to trigger the crowbar protection, the rotor side of the DFIG is shorted by the crowbar circuit and hence the rotor resistance is increased from Rr to Rrc. The flux coupling effect between the stator and rotor is enhanced as the rotor resistance is increased, that is to say σ_{rm} becomes

$$\sigma_{rmc} = \frac{R_{rc} L_m}{L_s L_r - L_m^2} \tag{19}$$

The new system matrix Ac can be obtained by replacing σ_{rm} with σ_{rmc}. As a result, are the two groups of characteristic roots of the stator rotor flux 4th order state equation.
For example, Figure 1 shows the relationship between the stator rotor flux and the crowbar resistance for a 2MW DFIGURE It is evident that the dynamic response of the stator and rotor flux will be influenced by the coupling effect between the stator and rotor flux. As the crowbar resistance decreases, σ_{sc} (or the stator transient flux attenuation rate) gradually increases. On the contrary, as the crowbar resistance increases, σ_{rc} (or the rotor transient flux attenuation rate) gradually increases. It is also important to note that $\sigma_{rc}$is far greater than σ_{sc}.

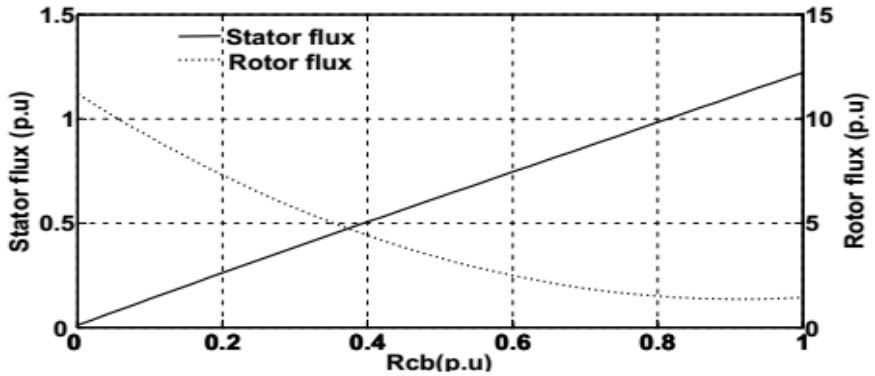

Figure 1: Relationship curve between the stator, the rotor and crowbar resistances.

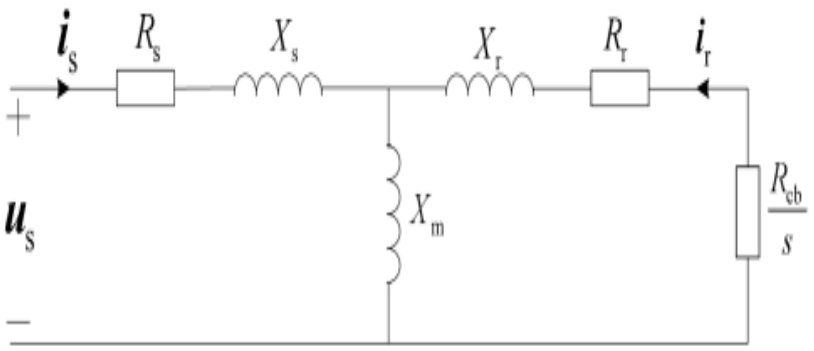

Figure 2: Impedance equivalent circuit of the DFIG with crowbar

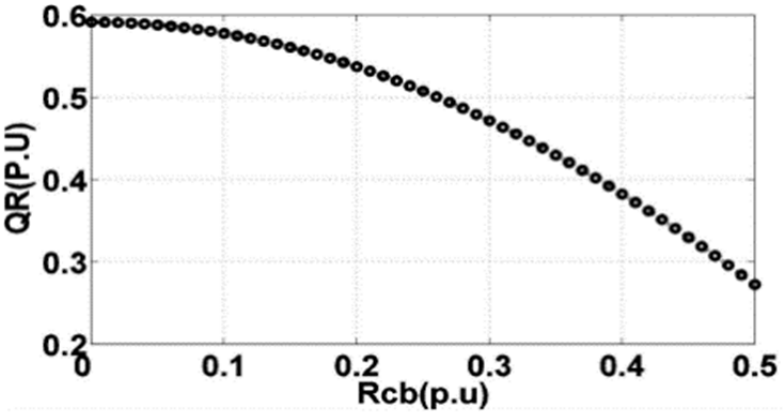

Figure 3: Relationship curve between the absorbed reactive power and the crowbar resistance

3.3 Impact on absorbing reactive power

When a voltage dip occurs, and the rotor overcurrent is large enough to trigger the crowbar protection, the DFIG may lose its controllability and behave as a squirrel-cage induction machine. The impedance equivalent circuit of the DFIG is shown in Figure 2, where Rcb is the crowbar resistance. Where, Rcb is crowbar reactance.

From Figure 2, the equivalent impedance of the DFIG with a crowbar can be described as:

$$Z = R + jX = (R_s + jX_s) + jX_m // (jX_r + R_r + \frac{R_{cb}}{s}) \tag{20}$$

where

$$R = R_s + \frac{\left(R_r + \frac{R_{cb}}{s}\right) X_m^2}{\left(R_r + \frac{R_{cb}}{s}\right)^2 + \left(X_m + X_r\right)^2}, \quad X = X_s + \frac{X_m\left[\left(R_r + \frac{R_{cb}}{s}\right)^2 + X_r\left(X_m + X_r\right)\right]}{\left(R_r + \frac{R_{cb}}{s}\right)^2 + \left(X_m + X_r\right)^2} \tag{21}$$

Ignoring the influence of the transient current, the steady state power of the DFIG (based on the relationship between active power and reactive power) can be written as

$$S = P + jQ = \frac{3}{2}\dot{U}_s \dot{I}_s^* = \frac{3}{2}U_s^2\left(\frac{R + jX}{R^2 + X^2}\right) \tag{22}$$

The reactive power that the DFIG absorbs or draws from the grid during a fault is then

$$Q_R = \frac{3}{2} U_s^2 \frac{X}{R^2 + X^2} \tag{23}$$

According to Eqn. (24), the reactive power draw is dependent on the stator voltage, the value of the crowbar resistance and the rotor speed of the DFIGURE

4. Verification of the theoretical analysis

A 3 MW DFIG connected to a power system network is simulated using MATLAB/SIMULINK software. The relevant parameters of the generator are given in the Appendix. The DFIG experiences a grid voltage sag of 80%, and this is sustained for a period of 625 ms. When the grid voltage sags, because the rotor overcurrent crowbar protection is in operation, the crowbar action lasts for around 100 ms. When the crowbar is cut off, the rotor converter is immediately restarted and provides reactive support to the grid. The simulated stator and rotor flux during the voltage sag, for different crowbar resistances, is shown in Figure 4 and Figure 5. From Figure 4, the amplitude of the stator flux is gradually reduced when the grid voltage sags at t=4s. However, with the increase in the crowbar resistance, the stator transient flux attenuation rate gradually decreases and this shows that the decay time constant of the stator flux DC component is reduced. From Figure 5, with an increase of crowbar resistance, the rotor transient flux attenuation rate gradually increases.

5. Conclusion

(1) During the process of DFIG LVRT, the value of the crowbar resistance is inversely proportional to the attenuation rate of the stator transient flux and proportional to the attenuation rate of the rotor transient flux. Large crowbar resistances can restrain the rotor transient current and reduce the reactive power that the DFIG absorbs from the grid effectively, but easily causes rotor overvoltage and the clamping effect of the DC bus. (2) In order to reduce the reactive power that the DFIG absorbs from the grid, an adaptive dynamic series capacitor is added in the crowbar circuit for the purpose of reactive power compensation. The proposed method has been applied to a 3 MW DFIG LVRT. The results obtained by adding the additional capacitor prove that the proposed method causes the rotor overcurrents to have a smaller transient time constant, and results in a faster recovery speed for the grid fault.

Acknowledgment

This work was supported by National Nature Science Foundation of China, the Natural Science Basic Research Plan in Shaanxi Province of China (2014JM8347), the Technology transfer to promote engineering project of Xi 'an bureau of science and technology (CXY1347-4) and the Scientific Research Program Funded by Shaanxi Provincial Education Department (17JK0049), Baoji University of Arts and sciences research platform project (ZK16029, ZK16012).

References

Mohsen R., Mostafa P., 2010, Grid-fault ride-through analysis and control of wind turbines with doubly fed induction generators, Electric Power Systems Research, 80(2), 184-195, DOI: 10.1016/j.renene.2012.04.014

Mikel A., Modesto A., Aitor G., 2012, Neural control for voltage dips ride-through of oscillating water column-based wave energy converter equipped with doubly-fed induction generator, Renewable Energy, 48, 16-26, DOI: 10.1016/j.renene.2012.04.014

Vinothkumar K., Selvan M.P., 2011, Novel scheme for enhancement of fault ride-through capability of doubly fed induction generator based wind farms, Energy Conversion and Management, 52(7), 2651-2658, DOI: 10.1016/j.enconman.2011.01.003

Niiranen J., 2004, Voltage dip ride through of doubly-fed generator equipped with active crowbar, Nordic Wind Power Conference, 1501-1507.

Xu D., Wang W., Chen N., 2010, Dynamic characteristic analysis of doubly-fed induction generator low voltage ride-through based on crowbar protection, Proceedings of the CSEE, 30(22), 29-36, DOI: 10.1016/j.egypro.2012.01.239